Mechanical Testing of Micromolded Plastic Parts by Nanoindentation

Tatiana Zhiltsova,[1] **Bernardo Daga**,[2] **Patricia Frontini**,[2] **Victor Neto**,[1] **Mónica Oliveira**[1]
[1]*Centro de Tecnologia Mecânica e Automação (TEMA), Department of Mechanical Engineering, University of Aveiro, Campus Universitário de Santiago, Aveiro, 3810 - 193, Portugal*
[2]*Universidad Nacional de Mar del Plata, Av. J. B. Justo 4302, Mar del Plata, B7608FDQ, Argentina*

Weld lines occur when two melt streams are combined. They may result in purely cosmetic imperfections, but also may represent part failure if placed in an area on the plastic highly subjected to stress during service. Qualitative assessment of these structural and cosmetics defects is usually accomplished by conventional mechanical characterization, destructive by nature, such as tensile testing or dynamic mechanical analysis (DMA). Nanoindentation offers the possibility for quick quasi-nondestructive *in situ* testing, allowing for monitoring the changes that occur in the surface layer of a plastic micropart. In this study, a methodology for the assessment of the superficial properties: hardness (H) and reduced Young's modulus (E_r) of micromolded parts was developed. The microparts, molded from Polyoxymethylene with two different sets of processing conditions were tested throughout the entire length and in the vicinity of the welding line. The observed hardness (H) and reduced Young's modulus (E_r) suggest that there is a steady increase in both values along the weld line from the adjoining flow front point at the inner side of the micropart towards the outer edge. In addition, H and E_r were found out to vary consistently with the alterations induced by the processing conditions. POLYM. ENG. SCI., 00:000–000, 2017. © 2017 Society of Plastics Engineers

INTRODUCTION

Weld line formation is a well-known phenomenon occurring during the injection molding process of polymers, when two melt streams are combined. With quantities and locations inherently linked to the polymer flow pattern in the impression, weld lines, when located at the areas subjected to load in service, besides the cosmetic defects, may threaten the molded part structural integrity [1].

This is especially true for micromolded parts, where polymer's cooling rates may be rather excessive, resulting in slower flow front advancement, as the melt flows further from the gate, and subsequently deficient intermixing of the flow fronts at the weld line location [2, 3]. The latter may pose a potential risk to the visual appearance and structural integrity of the micromolded parts and therefore should be properly assessed and addressed. In several recent studies, it has been reported that the weld line position and its severity can be considered as an indicator of the polymer fluidity as the flow front progresses away from the gate part of the microimpression, otherwise not likely to be accessed [4, 5].

Correspondence to: T. Zhiltsova; e-mail: tvzhiltsova@ua.pt
DOI 10.1002/pen.24799
Published online in Wiley Online Library (wileyonlinelibrary.com).

Over the recent years, a number of techniques have been employed for qualitative and quantitative assessment of the weld line quality of micromolded parts. Tosello et al. applied an atomic force microscope for three-dimensional topographical characterization of the surface of the weld lines and an optical CMM (Coordinate Measuring Machine) for geometrical characterization of the shape of the weld lines towards establishing the impact of the injection molding processing conditions on the weld line morphology [5, 6]. A number of authors reported that the surface width of the weld line and V-notch profile can be also measured by surface profilometers moving its probe perpendicular to the weld line [7, 8].

However, the aforementioned approaches are either qualitative by nature or quantitative but distractive as the assessments of the weld line tensile strength is concerned [8–10].

To counteract this trend, nanoindentation testing seems to be a promising technique and, therefore, has been an object of increasing interest for quick quasi-nondestructive *in situ* testing, allowing to monitor the changes that occur in the surface layer of a plastic micropart and its microstructure, formed as a result of the thermo-mechanical history experienced by the material. The latter has enabled to establish the relationships between the process variables and product characteristics [11, 12]. At macroscale, some interesting findings, in this direction, have been reported, substantiating the validity of the microindentation technique for the assessment of the microhardness variation along the weld line of the macrosized PS and PC parts [13–15]. The same concept was applied to the assessment of welded joints in several polymers and metals [16–18]. It should be noted, however, that to the best of the authors' knowledge, no research has been reported regarding the implementation of the nanoindentation technique for the assessment of the mechanical properties at the weld line locations of micromolded parts.

This study attempts to develop a methodology for the assessment of the superficial properties: hardness (H) and reduced Young's modulus (E_r) of micromolded parts. The microparts, molded from POM with two different sets of processing conditions were tested by nanoindentation throughout the entire length of the welding line and in its vicinity. To complement this approach, the weld line severity (width) and position was assessed by optical microscopy aiming to evaluate the influence of the injection molding processing conditions.

It also should be mentioned that the assessment of the morphological characteristics of the weld line formation and polymer flow dynamic, presented here, is only a fragment of a more extensive study [19] containing more injection trials with the different processing conditions and polymeric materials. The study presented here highlights the usefulness and potential of

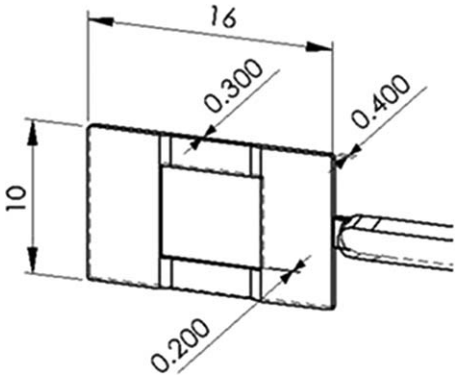

FIG. 1. Micropart's details (dimensions in mm).

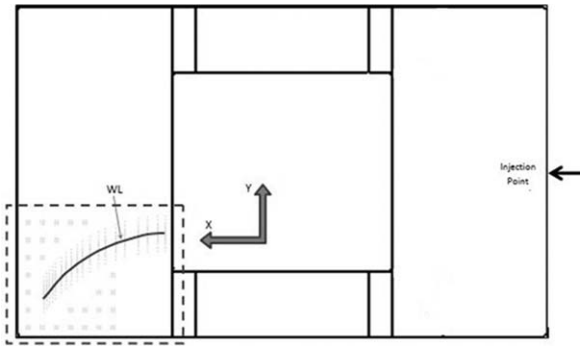

FIG. 2. Micropart's layout highlighting the indentation test pattern.

the developed nanoindentation technique and will be applied to the remaining of the data for further characterization.

EXPERIMENTAL SET UP

Experimental Equipment

The values of superficial hardness H and reduced Young's modulus E_r were determined as a function of the indenter's position using a triboindenter Hysitron TI900. The bright field optical imaging technique of Nikon Eclipse LV150 microscope was used for assessment of the weld line's shape, position and thickness.

Samples

The micropart under investigation features a 16 mm length by 10 mm width plate-like cavity with a central open space with the variable thickness of 200, 300, and 400 μm, as shown in Fig. 1.

To understand how the processing conditions might affect the strength of the weld lines in microparts, two samples were molded (Test 1) and (Test 2) under a particular range of the following processing conditions: barrel temperature (T_b), mold temperature (T_m), and injection speed (V_i), as presented in Table 1. Both samples were analyzed by tip indentation.

The samples (thickness of 400 μm) were cut from the micromolded parts, as depicted by the dotted line in Fig. 2. After cutting, the samples were glued onto a flat metallic sample holder. Finally, the samples surface was tested under the original conditions, i.e. without polishing and embedding.

Materials

The semi crystalline Polyoxymethylene Copolymer (POM) C 9021 by Ticona (Europe) with MFR of 8 g/10 min (190°C, 2.16 kg) was used for molding the microparts. As it has a substantially low moisture absorption rate and, POM did not require drying prior to processing. The choice of this polymer was also justified by the facility of the welding line visualization.

TABLE 1. Combination of the injection molding processing conditions.

Experiment N°	Melt temperature (°C)	Mold temperature (°C)	Injection velocity (mm/s)
Test 1	210	75	72
Test 2	250	95	144

Experimental Procedure

Load Function. In order to obtain a suitable depth of indentation, a Load Function (LF) was designed. This approach seeks to neutralize the influence of the surface roughness of the samples on the H and E_r measurements. LF has a maximum load of 9 mN and it has no hold time. The increase loading rate is 1.8 mN/s and the discharge rate is 90 mN/s. A maximum discharge load rate was selected in order to minimize the viscoelasticity effect and consequently the drift on hardness and modulus values. It is preferable not to use hold time to determine the influence of the injection molding processing conditions on mechanical properties through the entire length and in the vicinity of the welding line

Test Area. 19 indenting positions (columns) along the "visible" welding line were selected with the optical drive of the triboindenter through the entire length of the welding line, as shown in Fig. 3. Each column comprises 17 rows mounting to a total of 323 test pattern positions for indentation. In addition, to complete the characterization of the samples, more extra indentation positions were assigned, leading to the final pattern of 603 indentation positions for Test 2 and 723 for Test 1.

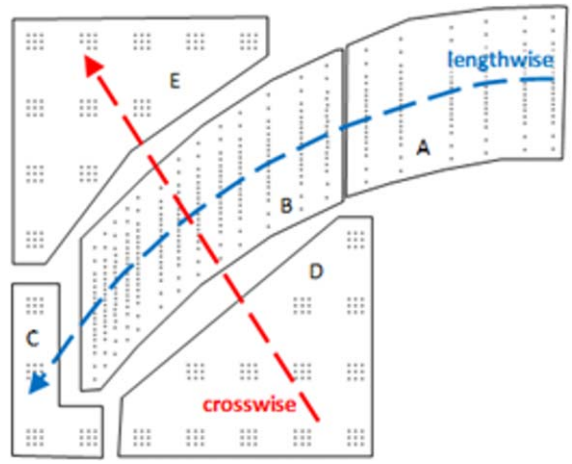

FIG. 3. Crosswise and lengthwise directions for Hardness and reduced Young's modulus analysis. [Color figure can be viewed at wileyonlinelibrary.com]

DOI 10.1002/pen

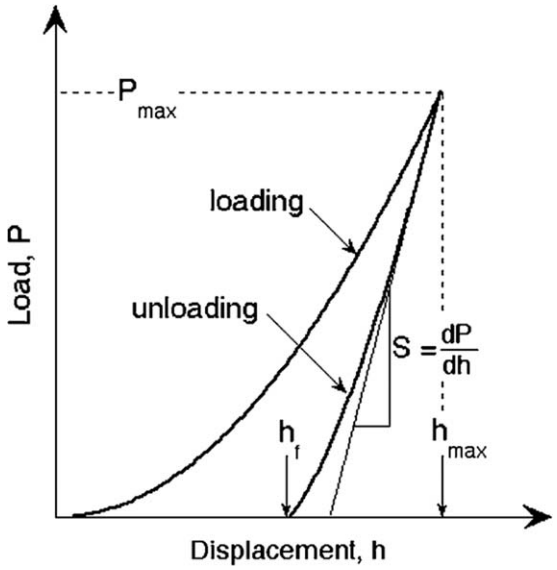

FIG. 4. Schematic illustration of indentation load –displacement data showing important measured parameters [21].

The directions chosen to analyze H and E_r results regarding their position to the weld line, i.e. crosswise and lengthwise are presented in Fig. 3.

As it can be seen, the indentations subgroups were identified by letters A–E, where A, B, and C are the subgroups in the lengthwise direction, while the crosswise direction encompasses subgroups D, B, and E.

Determination of Mechanical Properties

The indentation elastic modulus was determined as a function of indentation depth from the load–depth (P–h) curves (Fig. 4), using the approach outlined by Oliver and Pharr [20, 21].

This method is based on the assumption that the material behavior during unloading is purely elastic, and it is described as follows. The unloading part of the P–h curve is fitted through a power law function:

$$P = A(h - h_f)^m \tag{1}$$

and the contact stiffness (S) is calculated from the slope of the unloading curve as:

$$S = \frac{dP}{dh}\bigg|_{h_{max}} = mA(h_{max} - h_f)^{m-1} \tag{2}$$

where A and m are the power law function fitting parameters, h_f the residual penetration depth, and h_{max} are the maximum penetration depth achieved after the holding period.

The contact depth h_c is calculated by:

TABLE 2. Global values of H and E_r.

	Test1		Test 2	
Values	E_r (GPa)	H (GPa)	E_r (GPa)	H (GPa)
Mean	4.22	0.298	3.83	0.307
Std. Dev.	0.41	0.027	0.3	0.033

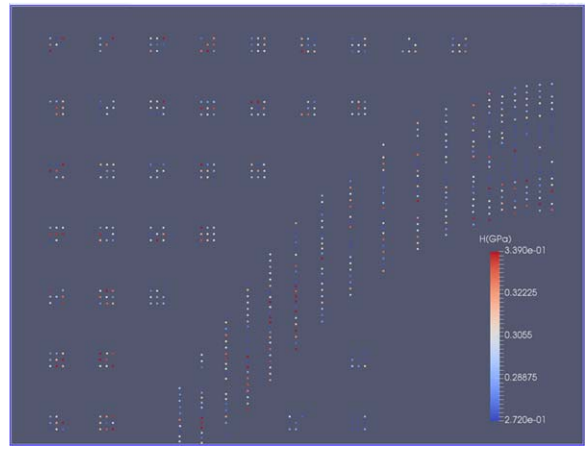

FIG. 5. Hardness as a function of position—Test 1. [Color figure can be viewed at wileyonlinelibrary.com]

$$h_c = h_{max} - \varepsilon\frac{P_{max}}{S} \tag{3}$$

where ε is a tip geometry factor, usually taken as 0.75. The reduced elastic modulus (E_r) was then calculated as:

$$E_r = \frac{S\sqrt{\pi}}{2\sqrt{A_c}} \tag{4}$$

where A_c is the actual contact area which accounts for the non-ideal shape of the tip. A_c was fitted to a polynomial function of h_c using a series of indentations performed on a fused quartz standard. E_r is directly related to the Young's modulus of the sample, E, by:

$$E_r = \left[\frac{1-v^2}{E} + \frac{1-v_i^2}{E_i}\right]^{-1} \tag{5}$$

where E_i and v_i are the Young's modulus and the Poisson's ratio of the indenter (1140 GPa and 0.07) while E and v are the sample properties.

Assessment of the Weld Line Width and Position

The bright field optical imaging technique of Nikon Eclipse LV150 microscope was chosen for visualization of the weld line

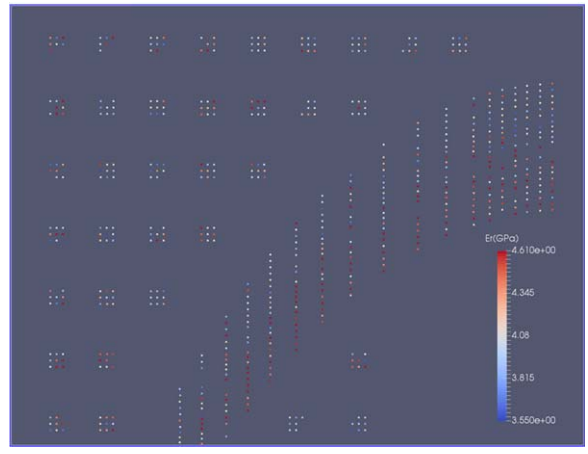

FIG. 6. E_r as a function of position—Test 1. [Color figure can be viewed at wileyonlinelibrary.com]

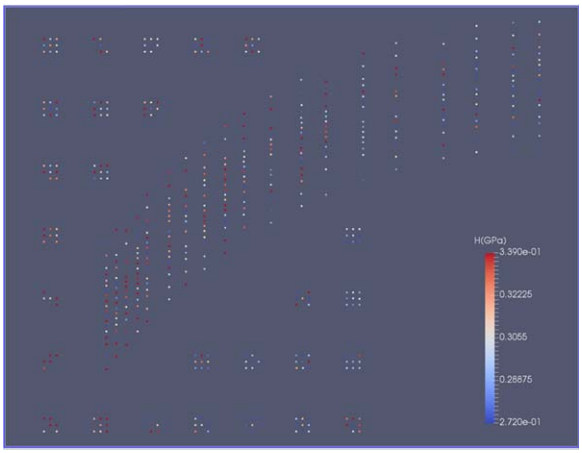

FIG. 7. Hardness as a function of position—Test 2. [Color figure can be viewed at wileyonlinelibrary.com]

width and position in POM microparts. For further processing and analysis, the images were recorded with a high quality digital camera, connected to the computer. Digitally stored images were calibrated for the assessment and subsequent quantitative comparison of the weld line position. The interior corner of the micropart, closest to the weld line (Fig. 2), was selected as an origin of measurements.

The weld line width was chosen as a quality signature of the microparts structural integrity being especially critical at the end of filling where POM fluidity may decrease as polymer melt rapidly cools. In order to assure statistical significance of the weld line width was assessed by undertaking measurements for ten randomly selected samples from the Test 1 and Test 2 injection molding runs.

RESULTS AND DISCUSSION

Assessment of Hardness H and Reduced Young's Modulus—E_r

Table 2 shows the H and E_r global mean values obtained by averaging all the measurements independently of their positions. It is evident that the two samples exhibit similar hardness while the difference in average modulus is of about 10%. However,

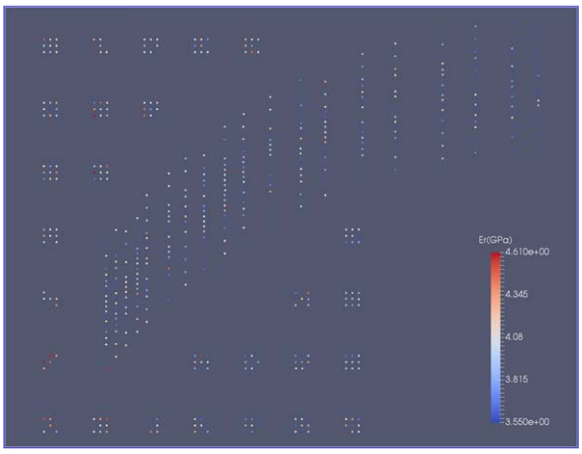

FIG. 8. E_r as a function of position—Test 2. [Color figure can be viewed at wileyonlinelibrary.com]

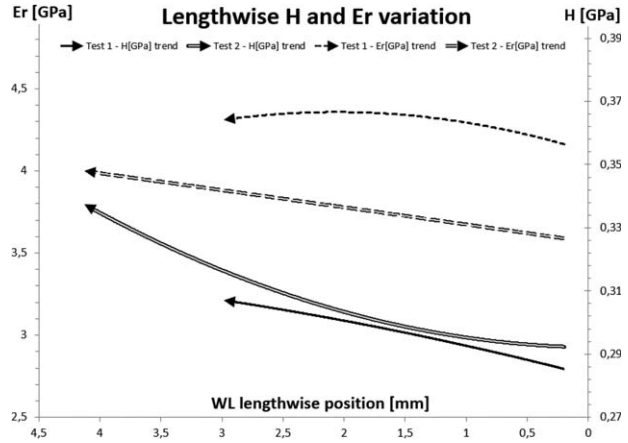

FIG. 9. Lengthwise (weld line) H and E_r variation (summary of the data depicted in Figs. 5–8).

the analysis of the global mean values appears to be restrictive and may hide valuable information.

Therefore, it is mandatory to analyze the distribution of the surface mechanical properties in the vicinity of the weld line at multiple positions. The values of H and E_r for the Test 1 (low values of the processing temperatures and injection velocity) are shown in Figs. 5 and 6, respectively.

While the hardness and E_r modulus of the micropart molded at higher mold and melt temperatures and injection velocity, corresponding to the Test 2, may be consulted from Figs. 7 and 8.

Given the rather extensive volume of data, the interpretation of Figs. 7 and 8 is getting more difficult. That is a reason why, the results were summarized in Figs. 9 and 10, reflecting the trends of the mechanical properties variations in the lengthwise and crosswise weld line directions, respectively.

In the case of Test 2, hardness is steadily increasing along the weld line (Fig. 9), being the lowest at the hypothetical point of the opposite flow fronts' encounter and then gradually rising as the fronts meet more obliquely, turning the weld line into a meld line. This trend is also applicable for the hardness variation along the Test 1 weld line, nonetheless, to a much lesser degree and with lower values. E_r is almost linearly rising along

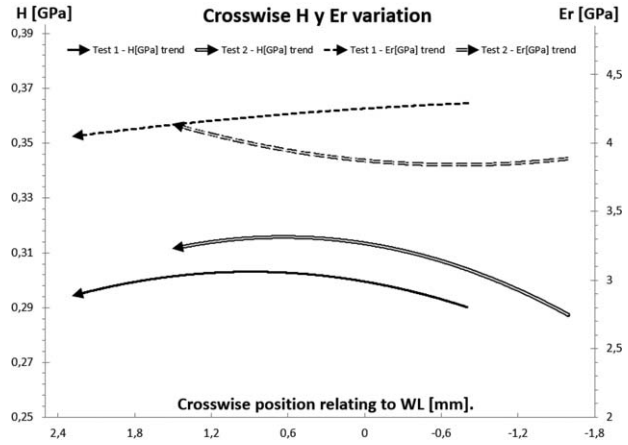

FIG. 10. Crosswise (weld line) H and E_r variation (summary of the data depicted in Figs. 5–8).

DOI 10.1002/pen

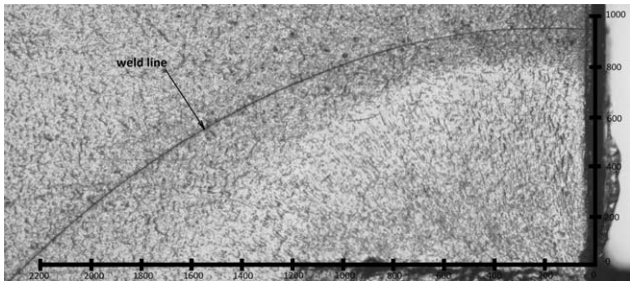

FIG. 11. The micrograph of the weld line fragment of POM—observed by optical microscopy (Test 1).

the weld line path for the Test 2, being, however, lower than the reduced elastic modulus of the Test 1 specimen, which in its turn, shows an imperceptible increase slightly parabolic in shape.

In what concerns hardness variation in the crosswise to the weld line direction (Fig. 10), it appears that the maximum values (on the top of the slightly parabolic curve) may be located in the close vicinity of the weld line, being an indicator of the appropriate polymer mixing during the meld line formation.

The E_r values of the Test 2 (crosswise to the weld line direction) are lower than that of the Test 1, but follow the increasing trend slightly parabolic in shape. However, the E_r of the Test 2, in spite of being higher than at the beginning, declines linearly at the same direction.

Assessment of Weld Line Width and Position

Pattern of the plastic as it enters the mold cavity is a key-factor for assessment of the polymer fluidity in a critical area of the microcavity such as the end of filling. It, therefore, may provide important information useful for understanding the influence of the processing conditions on the weld line formation. Figure 11 shows a micrograph of the weld line fragment in the POM micropart molded with the Test 1 processing conditions (Table 1), where its shape and position are clearly visible under a magnification of 5. As mentioned earlier, weld line's position is not symmetrical regarding its X axe (Fig. 2) and tends to be closer to thinner section side (200 μm), as depicted in Fig. 1, confirming the reduction of the polymer fluidity due to the cross-section restriction.

The averaged (ten randomly selected samples) weld line positions, from the Test 1 and Test 2, depicted in Fig. 12,

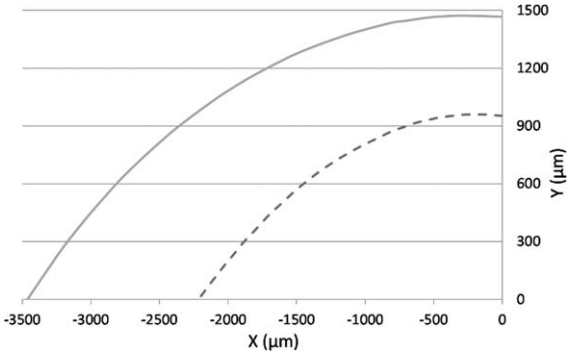

FIG. 12. Fragment of the averaged weld line location of POM for the experimental setups Test 1 (dashed line) and Test 2 (solid line).

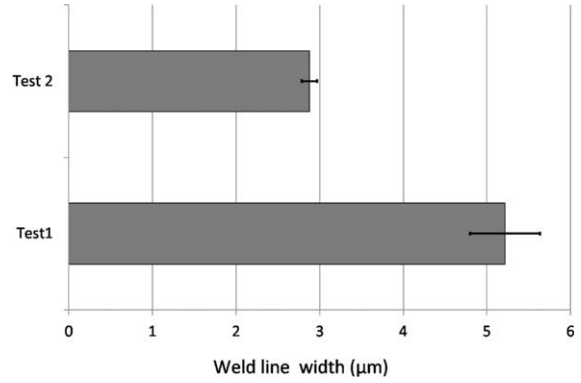

FIG. 13. Weld line width in POM microparts.

below, evidence the weld line advancement towards the center of the micropart with increase of the mold, melt temperatures and injection velocity. Moreover, considering a relatively small increase in the temperatures (Table 1), it is reasonable to assume that the injection velocity, which doubled from the Test 1 to the Test 2, is mainly responsible for such a significant advancement of polymer flow in the microcavity. This observation is in agreement with the results of Tosello et al. [5]. The indentation patterns, depicted in Figs. 5–8, also corroborate this statement.

Weld line severity was assessed in terms of its thickness. As expected, the weld line width in POM microparts (averaged value for 10 samples), shown in Fig. 13, decreases considerably from 5.2 μm (Test 1) to 2.9 μm (Test 2), being, therefore, a clear indication of the poorer polymer intermixing when molded with the Test 1 processing conditions. While drastic reduction in weld line width for Test 2 reflects a positive influence of higher mold and melt temperatures and faster injection velocity on the flow fronts interfusion and hence higher micromolded parts quality. It is also evident that variability of the injection molding process decreases at the higher levels of the processing conditions.

CONCLUSIONS

The methodology, based on nanoindentation testing, was developed and presented in this study. The results seem to be sensitive to the variation of the surface mechanical properties arisen from processing conditions of the micromolded parts. The main results may be summarized as follows.

- Reduced modulus values show significant variations as a function of the position, but not the reported hardness.
- Depending on the location and direction in respect to the weld line, different trends in surface mechanical properties were observed.
- Trends observed in the experimental mechanical properties are closely related with the injection molding processing conditions. The latter seem to be an indication of material anisotropy in the vicinity of the weld line, a fact that may be related to material fragility during a duty cycle.

The results also suggest that the injection velocity is the most significant factor for the E_r variation which positively correlates with slower injection velocity. Weld line width

measurements, performed by optical microscopy, indicated that the narrowest weld line width is related with high levels of the injection velocity, mold and melt temperatures, which contribute positively for intermixing of the polymer fronts and consequently, lessen the probability of microparts failure when subjected to mechanical solicitations. Moreover, a significant change in the weld line position was detected with the injection molding processing conditions at the upper level confirming once more improved polymer fluidity in the microcavity.

REFERENCES

1. D.V. Rosato and M.G. Rosato, *Injection Molding Handbook*, Springer, New York (2012).
2. T. Zhiltsova, M. Oliveira, and J. Ferreira, *J. Mater. Sci*, **48**, 81 (2013).
3. M.Oliveira, V. Neto, M. Fonseca, T.Zhiltsova and J.Grácio, *Microinjection molding of enhanced thermoplastics*, in *Thermoplastic Elastomers*, Rijeka, Croatia, Vol. **11**, InTech, 213 (2012).
4. T. Zhiltsova, M. Oliveira, J. Ferreira, J. Vasco, A. Pouzada, and A. Pontes, *Polym. Test*, **32**, 567 (2013).
5. G. Tosello, A. Gava, H.N. Hansen and G. Lucchetta, Influence of process parameters on the weld lines of a micro injection molded component. in Antec-Conference Proceedings, **4** (2007).
6. G. Tosello, A. Gava, H.N. Hansen, G. Lucchetta, and F. Marinello, *Wear*, **266**, 534 (2009).
7. C.-H. Wu, and W.-J. Liang, *Polym. Eng. Sci*, **45**, 1021 (2005).
8. L. Xie, and G. Ziegmann, *Microsyst. Technol*, **15**, 1427 (2009).
9. R. Seldén, *Polym. Eng. Sci*, **37**, 205 (1997).
10. G. Wang, G. Zhao, and X. Wang, *Mater. Des*, **46**, 457 (2013).
11. J. Chu, A. Hrymak and M. Kamal, Microstructural characteristics of micro-injection molded hermoplastics, in Antec-Conference Proceedings, **4**, 1985 (2007).
12. G. Greenway, P. Allan, and P. Hornsby, The characterisation and physical testing of micro-moldings. in ANTEC 2003 Conference Proceedings, 1995 (2003).
13. T. Nguyen-Chung, G. Mennig, M. Boyanova, S. Fakirov, and F.J. Baltá Calleja, *J. Appl. Polym. Sci*, **92**, 3362 (2004).
14. M. Boyanova, F.J. Baltá Calleja, S. Fakirov, I. Kuehnert, and G. Mennig, *Adv. Polym. Tech*, **24**, 14 (2005).
15. M.C. García, D.R. Gutiérrez Rueda, F.J. Baltá Calleja, I. Kühnert, and G. Mennig, *J. Mater. Sci. Lett*, **18**, 1237 (1999).
16. R. Lach, P. Hutař, P. Veselý, E. Nezbedová, Z. Knésl, T. Koch, C. Bierögel, and W. Grellmann, *POLIMERY-W*, **58**, 900 (2013).
17. S. Guangyong, X. Fengxiang, L. Guangyao, H. Xiaodong, and L. Qing, *Comp. Mater. Sci*, **85**, 347 (2014).
18. T.-H. Pham, and S.-E. Kim, *J. Constr. Steel Res*, **114**, 314 (2015).
19. T. Zhiltsova (2013). *Injection moulding process optimization for microstructured parts production* (Doctoral dissertation), Retrieved from RIA - Institutional Repository of the University of Aveiro http://hdl.handle.net/10773/12059.
20. W.C. Oliver, and G.M. Pharr, *J. Mater. Res*, **7**, 1564 (1992).
21. W.C. Oliver, and G.M. Pharr, *J. Mater. Res*, **19**, 3 (2004).

DOI 10.1002/pen